PHYSICAL REVIEW B **71**, 180411(R) (2005)

Reduction of the spin-wave damping induced by nonlinear effects

G. de Loubens, V. V. Naletov,* and O. Klein
Service de Physique de l'État Condensé, CEA Orme des Merisiers, F-91191 Gif-Sur-Yvette, France
(Received 22 February 2005; published 27 May 2005)

This paper reports a detailed measurement of M_z, the component parallel to the effective field direction, when ferromagnets are excited by microwave fields at high power levels. It is found that M_z drops dramatically at the saturation of the main resonance. Simultaneous measurements of M_z and absorption power show that this drop corresponds to a diminution of the spin-lattice relaxation rate. These changes are interpreted as reflecting the properties of longitudinal spin waves excited above Suhl's instability.

DOI: 10.1103/PhysRevB.71.180411 PACS number(s): 76.50.+g, 05.45.−a

The high power dynamics of magnetic structures is receiving much attention owing to the potential application to spin electronic devices. In this regime, the nonlinear (NL) contributions contained in the torque term of the gyroscopic equation become important as soon as the precession angle exceeds a couple of degrees. Although these effects were discovered in the ferromagnetic resonance (FMR) response of insulators,[1] they apply to every magnets. The same physics also occurs in metallic samples, as shown recently by An *et al.*[2] While the consequences of these nonlinearities on the microwave susceptibility have been thoroughly investigated,[3] their effects on M_z were not established.

This paper reports a measurement of M_z at the resonance saturation. We will present our data obtained at room temperature on an yttrium iron garnet (YIG) sample, shaped into a disk of diameter $D=160$ μm and thickness of 4.75 μm and uniformly magnetized by a static magnetic induction B_{ext} applied along the normal axis z of the disk.[4] It is found that M_z drops dramatically at the saturation of the main resonance. These findings indicate that the spin-lattice relaxation rate of the system decreases with increasing power. The change is interpreted as reflecting the properties of longitudinal spin waves (SW) excited above Suhl's instability. Because the butterfly curves of the nonlinear threshold in metallic samples also show a diminution of the damping for longitudinal spin waves,[2] it suggests that this diminution of the damping with increasing power is not specific to ferrites.

We exploit the exquisite sensitivity of magnetic resonance force microscopy (MRFM) to follow the changes in M_z with a resolution better than 1 ppm. A schematic of the setup is shown in Fig. 1(a). A cylindrical permanent magnet is glued at the free end of a clamped cantilever and then aligned with the axis of the YIG disk. The distance between the sample and the probe is fixed at 100 μm so that their coupling is in the weak interaction regime.[5] The inhomogeneous dipolar field generated by the sample creates a point load on the tip and thus an elastic deformation of the cantilever. Since the flexural modes of the cantilever are well below the Larmor frequency, the mechanical probe is insensitive to the precession of the transverse magnetization and it only couples to the longitudinal component M_z.

The measured quantity is $\Delta M_z = M_s - M_z$ when the microwave field is turned on. M_s is the saturation magnetization at the lattice temperature. The microwave is generated by a synthesizer and fed into an impedance matched stripline resonator tuned at $\omega_0/2\pi = 10.47$ GHz. We call h the circularly polarized amplitude of the microwave driving field at the sample position. If h is much lower than Suhl's threshold (see below) then the response is proportional to the excitation power. Figure 1(b) shows the FMR spectrum of our disk in the linear regime. A multiplicity of ΔM_z maxima are detected during a sweep of B_{ext}. The spectrum illustrates the quantized energy levels of magnetostatic waves (near-zero wave vector) confined by the sample diameter.

Simultaneously, we measure the imaginary part of the transverse susceptibility χ'' through a standard setup. The power reflected off the half-wavelength resonator is detected by a microwave crystal diode whose signal is proportional to the absorbed power $P_{\text{abs}} = \omega_0 \chi'' h^2$.

Although the discussion below can be extended to any of the magnetostatic modes above, we concentrate on the high power behavior of the main resonance at $B_0 = 5324.5$ G [see Fig. 1(b)]. This mode has a transverse wave vector $k_0 \approx \pi/D$ and is called hereof the uniform precession because it has no precessional nodes. We plot in Fig. 2 the microwave field dependence of χ'' (closed circles) and $\Delta M_z/h^2$ (open circles) evaluated at resonance. Both quantities are normal-

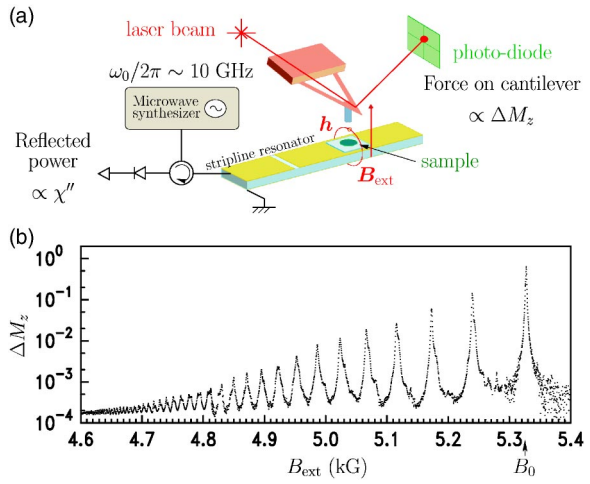

FIG. 1. (Color online) (a) Schematic of the experimental setup. A magnetic resonance force microscope is used to measure ΔM_z while a standard microwave setup measures χ''. (b) The linear FMR spectrum of the micron-size YIG disk detected mechanically. The main resonance occurs at B_0.

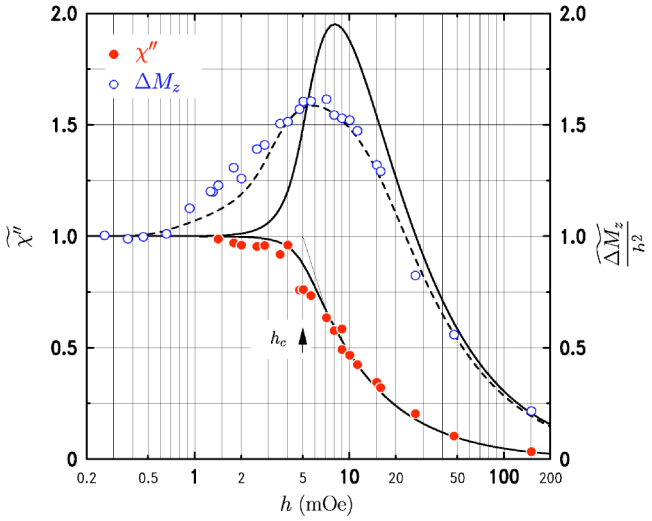

FIG. 2. (Color online) Microwave field strength dependence of the transverse (closed circles) and longitudinal (open circles) components of the magnetization at B_0. The quantities are normalized by their low power value. The solid lines are the analytical predictions (see text). The dashed line is the behavior corrected by finite-size effects.

ized by their low power values. The χ'' data shows the well-known premature saturation behavior above Suhl's threshold, $h_c=5$ mOe. Surprisingly, the power dependence of $\Delta M_z/h^2$ exhibits a peak at the threshold. Evidence of a behavior where $\Delta M_z/h^2$ increases with power has never been established before in any magnetic resonance experiment.

To gain further insight, we plot in Fig. 3 the ratio between the two measured quantities (the transverse and longitudinal component of the magnetization). We know from energy conservation arguments, that the power absorbed during the spin-lattice relaxation time, $\tau_1 P_{\text{abs}}$, must be equal to the energy stored in the sample, $\hbar\omega_0\Delta M_z/(\gamma\hbar)$. It implies that the ratio $\chi''h^2/\Delta M_z=1/(\gamma\tau_1)$ and Fig. 3 reveals the power dependence of the damping parameter. We find that the observed correlation between χ'' and $\Delta M_z/h^2$ corresponds to a monotonic diminution of the damping with increasing power. This ratio starts to decrease below h_c and the drop extends to the $h>h_c$ region.

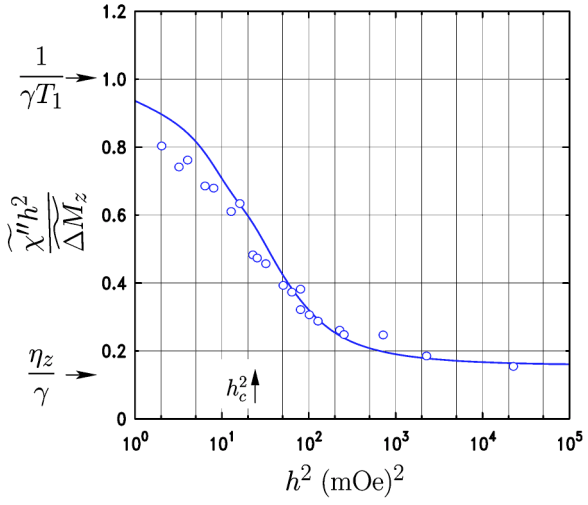

FIG. 3. (Color online) Power dependence of the ratio of χ'' over $\Delta M_z/h^2$. It measures the energy decay rate of the pumped spin-wave system. The solid line is the analytical prediction.

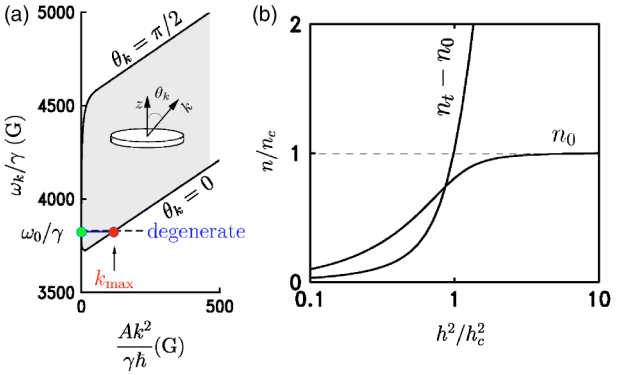

FIG. 4. (Color online) (a) SW dispersion: the shaded area is the magnon manifold explained in Ref. 6 (A is the exchange constant). (b) The power dependence of n_0 and n_t-n_0 for our sample.

The physics behind is best understood by decomposing the dynamics among the normal modes of the system. In particular, we consider the occupation of modes having identical energies ($\omega_k=\omega_0$) but different wave vectors ($k\gg k_0$) than the uniform mode. Degenerate modes exist because of the possible balance between exchange and demagnetizing energies. Figure 4(a) is the magnon manifold for our finite aspect ratio disk.[6] The exchange energy can increase by increasing k, while the demagnetizing energy of the SW mode can diminish by decreasing the angle θ_k between $\mathbf{k}$ (the propagation wave vector) and $\mathbf{M}_s$ (the magnetization vector). The shaded area represents the possible range of azimuthal angle $0\leqslant\theta_k\leqslant\pi/2$. The modes that are degenerate with the uniform precession lay on the horizontal line. We define n_k as the magnons' occupation number of the mode of wave vector k. Here we only count the magnons created by the microwave excitation. Thermal magnons' occupation numbers are accounted for in M_s and remain constant in all the measurements below. Assuming that each normal mode has a different energy decay rate to the thermodynamic equilibrium, η_k, then it is easy to show that $1/\tau_1$, the spin-lattice relaxation rate of the pumped system, equals to

$$\frac{1}{\tau_1}=\sum_{\{k\}}\eta_k\frac{n_k}{n_t}, \tag{1}$$

where $n_t=\Sigma_{\{k\}}n_k$. So the change in $1/\tau_1$ observed in Fig. 3 suggests that the relative weight n_k/n_t of the modes varies with power (NL effects) and that the high power regime favors modes having low relaxation rates. In our experiment, the transverse and longitudinal components of the magnetization reveal a different picture of the occupation of these modes. Short wavelength SW do not couple to χ'' because their transverse projection averages to zero. However, each magnon excitation diminishes the longitudinal component by $\gamma\hbar$. In other words, while the transverse data measures the number of uniform magnons $n_0=\frac{1}{2}\chi''^2h^2/(M_s\gamma\hbar)$, (occupation of the k_0 mode), the longitudinal data is proportional to

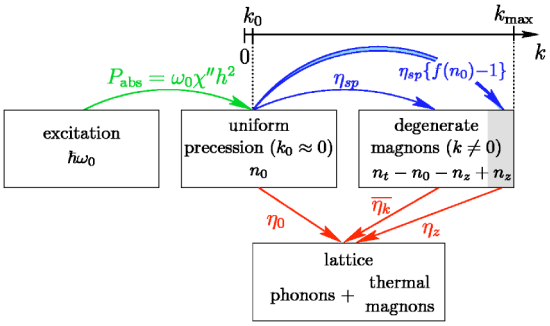

FIG. 5. (Color online) Block diagram of the energy transfers between the various degrees of freedom of the system. Transfers between the upper reservoirs conserve the total energy. The linear regime corresponds to $f(n_0)=1$. The shaded area and doubled line are the alterations by NL effects.

the total number of magnons $n_t=\Delta M_z/(\gamma\hbar)$. The NL terms that destroy the independence between degenerate modes were described by Suhl.[3] He found that, above a critical power (h_c^2), n_0 saturates at n_c as shown in Fig. 4(b) and this saturation is associated with a surge of parametric magnons propagating at $\theta_k=0$.

Before proceeding further, we need to look more specifically at the different relaxation channels in our sample. These damping forces are necessary to stabilize the SW excited by the nonlinearities.[3] Figure 5 establishes a schematic of the coupling between the various degrees of freedom in the system. At ω_0 and B_0, the uniform microwave field preferentially couples to the uniform mode, the longest wavelength mode available inside the degenerate band. Its energy relaxation rate directly to the lattice will be written η_0 (our definition is twice as large as the amplitude relaxation rate used in Suhl's paper[3]). The linewidth of the peaks in Fig. 1(b), however, is the sum $(\eta_0+\eta_{sp})/\gamma$, where η_{sp} is the decay constant of the uniform precession to degenerate SW due to scattering on the sample inhomogeneities. We define $\overline{\eta_k}$ as the average decay rate to the thermodynamic equilibrium of the degenerate magnons. Translated into Bloch's notation, the linear part of the diagram in Fig. 5 corresponds[7] to $T_2=2/(\eta_0+\eta_{sp})$ and $\tau_1(h\ll h_c)=T_1=(T_2/2)(1+\eta_{sp}/\overline{\eta_k})$, respectively, the transverse and longitudinal relaxation times in the linear regime. These relaxation times, in the limit of infinitesimal excitations, have been completely characterized in a previous paper.[8] Their values are summarized in Table I.

The NL terms in the gyroscopic equation[3] couple coherently degenerate SW of equal and opposite wave vectors $(+\mathbf{k},-\mathbf{k})$. The coupling to the uniform motion, $\xi_k n_0$, depends on θ_k and it is maximum $(\xi_k|_{max}/\gamma=2\pi M_s\approx 900$ G) for longitudinal SW ($\theta_k=0$). We use Suhl's notation for ξ_k so that the reader can refer to Ref. 3 for a complete treatment. In our disk, these SW have a wave-vector $k_{max}\approx 6.3\times 10^4$ cm^{-1} [see Fig. 4(a)]. A critical threshold is reached when $\xi_k n_0$ becomes comparable to η_z, the relaxation rate to the lattice of the longitudinal SW. Two quanta of the uniform precession then break down in a parametric magnon pair propagating along $\mathbf{M}_s$. The instability corresponds to a spatial distortion of the instantaneous axis of precession, which diminishes the transverse demagnetizing energy. The critical number of uniform magnons is $n_c=\frac{1}{2}(\gamma M_s T_2^2 h_c^2/\hbar)$ with $h_c^2=\eta_z/(2\gamma^2 T_2^2\xi_k)$, the saturation power. In FMR, the alteration of the energy flow between the modes can be summarized as shown in Fig. 5.

$$\frac{\partial}{\partial t}n_0=\frac{P_{abs}}{\hbar\omega_0}-\{\eta_0+\eta_{sp}f(n_0)\}n_0 \tag{2a}$$

$$\frac{\partial}{\partial t}(n_t-n_0-n_z)=\eta_{sp}n_0-\overline{\eta_k}(n_t-n_0-n_z) \tag{2b}$$

$$\frac{\partial}{\partial t}n_z=\eta_{sp}\{f(n_0)-1\}n_0-\eta_z n_z, \tag{2c}$$

where $f(n_0)=1/\sqrt{1-n_0^2/n_c^2}$ (Ref. 9) and n_z is the number of parametric magnons.

In the stationary regime, Eq. (2a) leads to an implicit equation for the susceptibility derived by Suhl[9]

$$\widetilde{\chi''}=\frac{\eta_0+\eta_{sp}}{\eta_0+\eta_{sp}/\sqrt{1-\widetilde{\chi''}^4(h/h_c)^4}}, \tag{3}$$

where $\widetilde{\chi''}=\chi''/(\gamma T_2 M_s)$ is the susceptibility normalized by its low power value. We try to compare quantitatively our data to the profile predicted by Eq. (3). We use the measured value of the threshold, $h_c=5$ mOe, in the formula. It corresponds to $\eta_z/\gamma=0.15$ G, a value consistent with previous measurements in spheres and thin plates,[10] where it was found that the decay rate becomes smaller as θ_k diminishes.[7,10] We have displayed in Fig. 2 the predicted behavior, with no fitting parameters. The model properly predicts the shape and the smearing out of the singularity at h_c.

Solving the set of Eq. (2) in the steady state gives a new analytical relationship between χ'' and $\Delta M_z/h^2$

$$\widetilde{\frac{\Delta M_z}{h^2}}=\widetilde{\chi''}+\left(\frac{1}{T_1\eta_z}-1\right)\{\widetilde{\chi''}-\widetilde{\chi''}^2\}, \tag{4}$$

where $\widetilde{\Delta M_z}=\Delta M_z/(\gamma^2 T_1 T_2 M_s)$ is normalized by the slope of $\Delta M_z/h^2$ at low power. The above equality is equivalent to an energy balance between the absorbed power and the dissipated power in the sample $P_{abs}=P_{diss}=\hbar\omega_0\Sigma_{\{k\}}\eta_k n_k$.[7,11] The solid line in Fig. 2 is the bell-shape behavior inferred from Eq. (4) with values of η's of Table I. Experimentally we find that the raise of $\Delta M_z/h^2$ begins at powers lower than h_c. We have omitted in our model the finite-size effects in order to keep the discussion simple. But the so-called uniform mode has a spatially dependent precession amplitude. ΔM_z at the center of the disk is about three times larger than its spatial

TABLE I. Relaxation rates of degenerate magnons (in gauss).

spin-spin process	uniform precession	kth magnons	longitudinal magnons
η_{sp}/γ	η_0/γ	$\overline{\eta_k}/\gamma$	η_z/γ
0.2	1.07	0.65	0.15

average.[4] Changes in the profile are expected when different locations of the sample hit the saturation threshold. While the raise of $\Delta M_z/h^2$ coincides with the saturation of the central part of the disk, the spatially averaged transverse susceptibility χ'' drops at higher power, approximately when the periphery saturates (zone with the highest spatial weight). The dashed line in Fig. 2 is the predicted behavior when Eq. (4) is weighted by the spatial profile of ΔM_z. Such good agreement with the data suggests that the shift of the peak towards $h<h_c$ is due to these finite-size effects. We note that these spatial dependences are further magnified by the MRFM technique, which provides a local measurement (here the mechanical probe is above the disk center).

Our model explains also simply the results in Fig. 3. The relaxation rate $1/\tau_1$ in Eq. (1) is simply equal to $1/T_1$ when $f(n_0)=1$ (linear regime) and then it reduces to η_z when $f(n_0)\gg 1$. The two limits correlate respectively to $n_t \approx n_0$ and $n_t \approx n_z$. The solid line in Fig. 3 is the drop inferred from the analytical expression showing how the η_z value is approached asymptotically. We find that the agreement with the data extends well above h_c and the asymptotic value is in agreement with the η_z inferred from the threshold value, h_c. We recall that our model only considers the NL coupling between the uniform and the longitudinal magnons. A proper analysis, however, should also account for the NL coupling between all the degenerate modes, which become important at much higher powers. They correspond to a different redistribution of the degenerate magnons' occupation number in the flow diagram of Fig. 5.

In conclusion, this paper studies the changes of properties of excited SW due to NL effects. If the excitation mechanism favors a particular mode, then a four-magnon process starts at high power levels to redistribute the magnons' occupation number between degenerate modes. During the redistribution, the coupling to the excitation usually decreases: less energy is absorbed for the same excitation energy. The efficiency, however, increases because the newly filled modes (the longitudinal ones[6]) have lower energy relaxation rates: more SW are emitted for the same absorbed energy. Recent measurements in metallic samples also show a diminution of the damping for longitudinal spin waves,[2] which suggests that this diminution of $1/\tau_1$ with increasing power is not specific to ferrites. These results are important because they challenge some of the assumptions used in the Landau-Lifshitz-Gilbert equation to simulate the high power dynamics. Finally, we emphasize the importance of doing a direct measurement of the damping. It is known that linewidth increases in the NL regime because of foldover effects.[4] These high power effects are thus an illustration of a case where an increased linewidth coincides with a diminution of the damping.

We are greatly indebted to J. Ben Youssef, V. Charbois, M. Viret, X. Waintal, C. Fermon, and O. Acher for their help and support. This research was partially supported by the E.U. project M^2EMS (IST-2001-34594) and the Action Concertée Nanoscience NN085.

*Also at Physics Department, Kazan State University, Kazan 420008, Russia.

[1] R. W. Damon, Rev. Mod. Phys. **25**, 239 (1953).
[2] S. Y. An, P. Krivosik, M. A. Kraemer, H. M. Olson, A. V. Nazarov, and C. E. Patton, J. Appl. Phys. **96**, 1572 (2004).
[3] H. Suhl, J. Phys. Chem. Solids **1**, 209 (1957).
[4] V. V. Naletov, V. Charbois, O. Klein, and C. Fermon, Appl. Phys. Lett. **83**, 3132 (2003).
[5] V. Charbois, V. V. Naletov, J. Ben Youssef, and O. Klein, Appl. Phys. Lett. **80**, 4795 (2002).
[6] M. Sparks, *Ferromagnetic Relaxation Theory* (McGraw-Hill, New York, 1964).
[7] R. C. Fletcher, R. C. LeCraw, and E. G. Spencer, Phys. Rev. **117**, 955 (1960).
[8] O. Klein, V. Charbois, V. V. Naletov, and C. Fermon, Phys. Rev. B **67**, 220407 (2003).
[9] H. Suhl, J. Appl. Phys. **30**, 1961 (1959).
[10] C. E. Patton and W. Jantz, J. Appl. Phys. **50**, 7082 (1979).
[11] E. Schlömann, Phys. Rev. **116**, 828 (1959).